Available online at www.sciencedirect.com

ScienceDirect

Procedia Structural Integrity 37 (2022) 525–532

Structural Integrity Procedia

www.elsevier.com/locate/procedia

ICSI 2021 The 4th International Conference on Structural Integrity

On the defect tolerance by fatigue spectral methods based on full-field dynamic testing

Alessandro Zanarini*

DIN, Industrial Engineering Dept., University of Bologna, Viale Risorgimento 2, 40136 Bologna, Italy

Abstract

In real life production of dynamically loaded components, we might accept the risk of defects only if we can assess their position by NDT techniques, their effect by proper cumulative damage theory, the dynamic signature of the excitation and the structural dynamics of our structures in service. This work addresses the latter topic by means of experimental full-field optical techniques, which can provide accurate surface displacement distribution in a broad frequency band directly from real components, while recording the excitation, thus, with advanced numerical derivations, coming to an experiment-based full-field strain FRF characterisation, here applied on an aluminium plate. The knowledge of the material constitutive parameters is used to obtain the Von Mises equivalent stress FRFs. The signature of the excitation permits the evaluation of the Von Mises stress PSDs, which can be used in a spectral fatigue method (here the one from Dirlik), coming to a frequency-to-failure distribution. The same distribution can be scaled to a risk index and compared to the defect locations from NDT, in order to build a defect tolerance map and discriminate the product acceptance for dynamically loaded components. The smart exploitation of full-field optical techniques play a relevant role in measuring, with high spatial resolution, the manufactured components in their effective broad structural dynamics and give defect tolerance experiment-based maps, without the need of a highly tuned FE model.

Peer-review under responsibility of Pedro Miguel Guimaraes Pires Moreira

Keywords: defect tolerance; optical full-field dynamic testing; full-field FRFs; fatigue spectral methods; NDT

1. Introduction

The key idea sketched in this brief article is to use a broad frequency band *experiment-based full-field FRF approach* to bring the complete & real structural dynamics into fatigue life expectations, which come as failure maps, therefore opening for a risk tolerance strategy of the defects that may be inside the material, due to the manufacturing process or to excessive loading. In such a broad perspective, for the retained dynamics and for the high resolution mapping achievable, the location of the potential defect plays an uttermost relevance in the crack & failure start: what follows is devoted to highlight the potentials of this smart approach with simple examples.

* Corresponding author. Tel +39 051 209 3442.
E-mail address: a.zanarini@unibo.it (Alessandro Zanarini).

Peer-review under responsibility of Pedro Miguel Guimaraes Pires Moreira
10.1016/j.prostr.2022.01.118

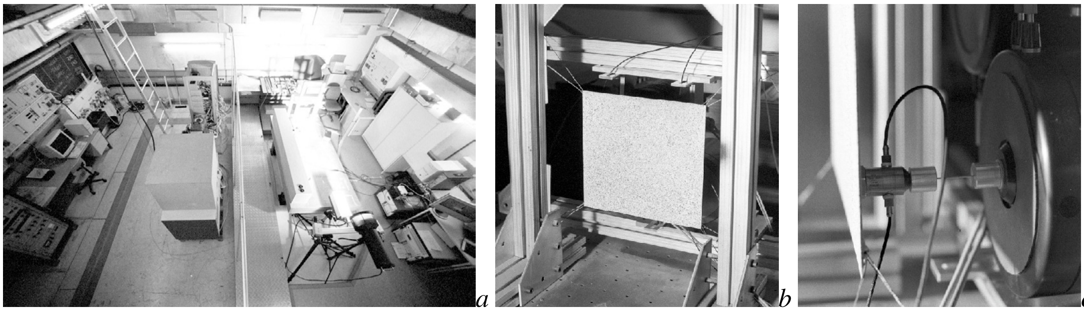

Fig. 1. The lab in the TEFFMA project Zanarini (2014a,b, 2015a,b,c,d, 2018, 2019a,b, 2021c): aerial view in *a*, restrained plate sample in *b*, 2 shakers on the back of the plate in *c*.

It is important to remark how these works, about direct experimental models from optical measurements, are based on: non-contact measurements, no structural dynamics distortions, dense grid of sensing locations; broad frequency band experimental vibration model with accurate spatial description for complex pattern identification; experimental dynamic model for strains, stresses & failure criteria; accurate maps of cumulative damage distributions for fatigue life assessment; defect tolerance criteria and risk index based on full-field testing in production & working conditions.

These works are a spin-off of the activities held during the *Towards Experimental Full-Field Modal Analysis* (TEFFMA) project, after the grown seeds put in the HPMI-CT-1999-00029 *Speckle Interferometry for Industrial Needs* Post-doctoral Marie Curie Industry Host Fellowship project at Dantec Ettemeyer GmbH. Since the testing in the latter (see Zanarini (2005a,b)) it became self-evident how ESPI measurements could give relevant mapping about the local behaviour for enhanced structural dynamics assessments (see Zanarini (2007)) and fatigue spectral methods (see Zanarini (2008a,b)). The results in the former were the basis for the TEFFMA birth, whose works saw earlier presentations in Zanarini (2014a,b), followed by Zanarini (2015a,b,c,d). In Zanarini (2018) a gathering of the works of TEFFMA was firstly attempted, while in Zanarini (2019a) an extensive description of the whole receptance testing was faced and in Zanarini (2019b) the EFFMA was detailed together with model updating attempts. The works in Zanarini (2020) underlined the quality of ESPI datasets in full-field dynamic testing. In Zanarini (2021c) a precise comparison was made about new achievements for rotational and strain FRF high resolution maps.

A brief description of the testing is outlined in Section 2 , with attention on the set-up, on the topology transforms needed for comparisons and on the obtained raw results. Section 3 deals with the numerical derivation of strain and stress fields from receptance maps, which are relevant to the cumulative damage spectral methods in Section 4. Section 5 pertains the selection of a defect tolerance scheme, before Section 6 for the final conclusions.

2. The testing for the TEFFMA project

2.1. Brief summary of the technological equipment

To the interested reader, the most detailed test campaign appeared in Zanarini (2019a), with further suggestions in Zanarini (2019b, 2020, 2021c), but here is a brief summary of what was available at TU-Wien as in Fig.1: a dedicated room with a seismic floor; a mechanical and electronic workshop with technicians at disposal; traditional tools for vibration & modal analysis; but, in particular, there were SLDV, Hi-Speed DIC and ESPI measurement instruments.

Accurate studies were needed to understand each technological limit and if a common test for concurrent usage might have been really possible. All this brought to a unique set-up for the comparison of the 3 optical technologies in full-field FRF measurements; great attention was paid on the design of experiments for further research in modal analysis.

After an accurate tuning, a feasible performance overlapping was sought directly out of each instrument, reminding that the same structural dynamics can be sensed in complementary domains, which means frequency for SLDV & ESPI, time for DIC. The comparisons of the Operative Deflection Shapes, directly out of each instrument proprietary software, seem really promising, thanks to the high quality achieved in the results, but it can be easily understood that only qualitative comparisons are possible at this early stage, as nothing is precisely super-imposable.

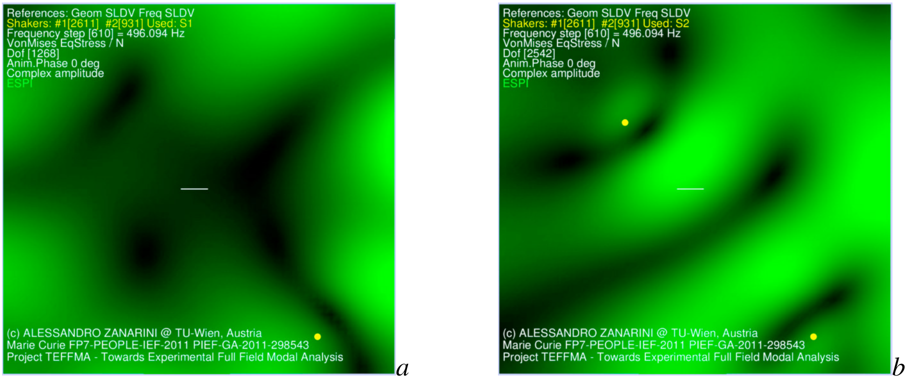

Fig. 2. Examples of *Von Mises equivalent stress FRF maps* from optical techniques, direct experimental impedance models at 496 Hz, ESPI examples: from shaker 1 in *a*, from shaker 2 in *b*.

2.2. Topology transforms for quantitatively comparable results

A methodology, a comparative paradigm is therefore needed to have quantitative & sound comparisons, in the shape of a topology transform methodology. The methodology was based on the identification of two shakers' points on each dataset, then proceeded to scale, rotate and align the grids to a unique 2D coordinate system. The common portion of the measured area was extracted via discrete geometry reductions.

2.3. Estimated full-field FRFs & Coherence from optical measurements

Once the methodology above is defined, function (*receptance FRF & Coherence* functions) maps at specific frequencies and excitation sources can be obtained as in Zanarini (2019a), to appreciate the spatial consistency & continuity of the data, with clean shapes, sharp nodal lines and excellent *Coherence*, especially from ESPI. Each of these transformed dataset is precisely comparable with the others, up to the numerical precision of the topology transforms.

3. Deriving new quantities from full-field receptances

The high quality of these *receptance maps* deserves further investigations for novel derivative quantities, starting from highly detailed strain maps.

3.1. Dynamic Strain FRFs

By means of a robust differential operator (see in particular Zanarini (2021c)) on the *receptance map* $\mathbf{d}(x, y, j\omega)$ along x & y directions, the *full-field generalised strain FRFs* can be obtained in each map location and frequency line:

$$\varepsilon(x,y,j\omega)_{ik} = \frac{1}{2}\left(\frac{\partial \mathbf{d}(x,y,j\omega)_i}{\partial q_k} + \frac{\partial \mathbf{d}(x,y,j\omega)_k}{\partial q_i}\right), \tag{1}$$

as well as the *strain tensor* components due to out-of-plane bending-related displacements of the plate of thickness s:

$$\varepsilon(x,y,j\omega)_{xx_b} = -\frac{s}{2}\frac{\partial^2 \mathbf{d}(x,y,j\omega)_z}{\partial x^2},\ \varepsilon(x,y,j\omega)_{yy_b} = -\frac{s}{2}\frac{\partial^2 \mathbf{d}(x,y,j\omega)_z}{\partial y^2}, \gamma(x,y,j\omega)_{xy_b} = \gamma(x,y,j\omega)_{yx_b} = -s\frac{\partial^2 \mathbf{d}(x,y,j\omega)_z}{\partial x \partial y}. \tag{2}$$

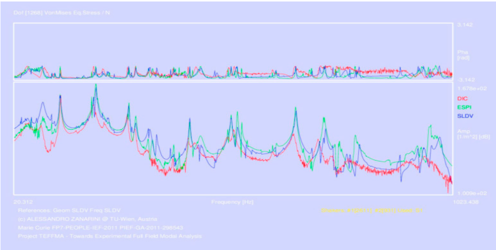
a

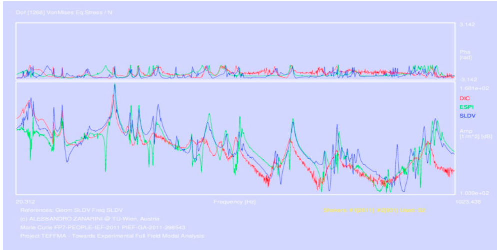
b

Fig. 3. Examples of *Von Mises equivalent stress FRF graphs* from optical techniques, direct experimental impedance models in the 20-1024 Hz range, DIC-ESPI-SLDV examples: from shaker 1 in *a*, from shaker 2 in *b*.

Also the *Principal Strain FRF maps*, from both shakers, can be obtained at each frequency line of the domain, with a complex-valued data representation, to retain any phase relation: it becomes an impressive characterisation of the experiment-based strain distribution over the sensed surface in spatial and frequency domains.

3.2. Dynamic Stress FRFs

Having worked on examples from an aluminium sample in Fig.1*b*, with the introduction of a linear isotropic constitutive model (with the following material parameters: E elastic modulus, ν Poisson ratio, G shear modulus, Λ Lamé constant), the *Stress FRF tensor* components can be evaluated from *Strain FRFs*:

$$\begin{aligned}\sigma_\omega(x,y)_{ii} &= 2G\varepsilon_\omega(x,y)_{ii} + \Lambda\left(\varepsilon_\omega(x,y)_{xx} + \varepsilon_\omega(x,y)_{yy}\right)\\ \sigma_\omega(x,y)_{ij} &= 2G\varepsilon_\omega(x,y)_{ij}\\ G = E/2\,(1+\nu);\ \Lambda &= E\nu/((1+\nu)\,(1-2\nu))\end{aligned} \tag{3}$$

Therefore, with the constitutive model of any specific material (anisotropic and locally linearised included), also the *experiment-based Principal Stress FRF maps* can be evaluated from the *full-field receptances*.

4. Cumulative damage in fatigue life assessment

With such a broad set of detailed *experiment-based Stress FRF maps*, we can evaluate cumulative damage with the *spectral methods* for high cycles fatigue in every dof of the sensed surface, with an *unprecedented mapping ability*.

4.1. Spectral method parameters

Thanks to the *full-field FRFs*, we can approach the cumulative damage estimation by means of any *spectral method* in each location (x, y) of the maps, which targets the evaluation of an *equivalent range of stress cycles* $S_{eq}(x, y)$, representative of the damage inferred by the whole spectrum of the retained dynamics.

The *spectral methods* are based on $m_k = \int_0^\infty f^k PSD_{VM}(\omega)d\omega$, the *k-th order moments* of the frequency by the *power spectral density (PSD)* of *Von Mises equivalent stress* $PSD_{VM}(\omega)$, from which we can obtain other parameters, such as the *effective frequency* $F_{zerocrossing} = F_{zc} = \sqrt{m_2/m_0}$, the *expected number of peaks per unit time* $F_{peaks} = F_p = \sqrt{m_4/m_2}$, and the *irregularity factor* $\gamma = \gamma_2 = F_{zc}/F_p = m_2/\sqrt{m_0 m_4}$.

4.1.1. Dirlik semi-empirical spectral method parameters

Among the many available (see Dirlik and Benasciutti (2021)), the *Dirlik semi-empirical spectral method* in Dirlik (1985) was here implemented, as it gives a sound prediction of the fatigue life for wide-frequency-band spectra of

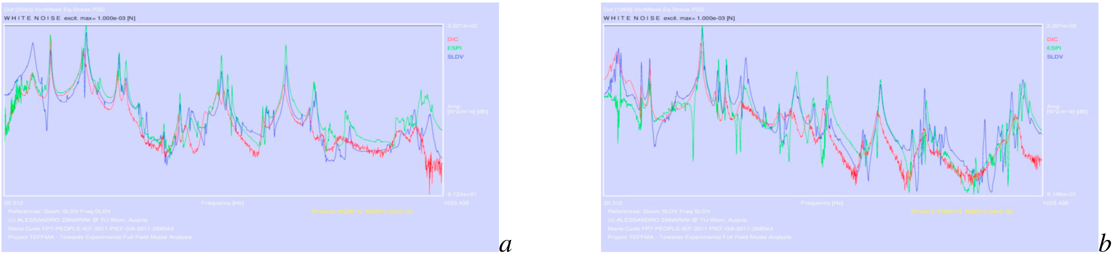

Fig. 4. Examples of *white noise Von Mises equivalent stress PSD* graphs from optical techniques, direct experimental impedance models in the 20-1024 Hz range, DIC-ESPI-SLDV examples: from shaker 1 in *a*, from shaker 2 in *b*.

stress responses, combining the factors in Eq.4:

$$\chi_m = (m_1/m_0)(m_2/m_4)^{1/2};\, D_1 = 2\left(\chi_m - \gamma^2\right)/\left(1+\gamma^2\right);\, R = \left(\gamma - \chi_m - D_1^2\right)/\left(1 - \gamma - D_1 + D_1^2\right)$$
$$D_2 = \left(1 - \gamma - D_1 + D_1^2\right)/(1-R);\, D_3 = 1 - D_1 - D_2;\, Q = 1.25\,(\gamma - D_3 - D_2 R)/D_1; \tag{4}$$

to finally obtain the *Equivalent Range of Stress Cycles* $S_{eq}(x,y)$ raised to b exponent

$$S_{eq}^b = D_1(2\sqrt{m_0}Q)^b\Gamma(b+1) + (2^{3/2}\sqrt{m_0})^b\Gamma(1+b/2)[D_2R^b + D_3], \tag{5}$$

and the *Time-to-Failure distribution* in:

$$T_{failure}(x,y) = K_r/\left(F_p(x,y)S_{eq}^b(x,y)\right). \tag{6}$$

function of $S_{eq}(x,y)$, of $F_p(x,y)$ and of the K_r fatigue strength coefficient and b exponent. Please note that the *Time-to-Failure distribution* is evaluated across all the dofs (x,y) of the maps.

4.2. The role of Von Mises equivalent stress FRFs from optical techniques

The *PSD of Von Mises equivalent stress* is crucial and evaluated from the *Von Mises equivalent stress FRFs*, here rendered in the maps at a single frequency in Fig.2 and in single dof graphs of Fig.3, from both shakers.

Important to note is that the *experiment-based full-field stress FRFs* are usable with any other spectral method (see e.g. Dirlik and Benasciutti (2021)), in particular those that retain the phase relations in the frequency domain, for further comparative works.

4.3. Frequency-to-failure with coloured noise excitation

As in Zanarini (2015c, 2018) new *PSDs* are easily obtained from the *stress FRFs*, when changing the *excitation signature*. By selecting the *white noise* excitation to multiply the previous *stress FRFs*, the *PSDs* of *Von Mises equivalent stress maps* (shown in single dofs in Fig.4) are used to give the reciprocal of Eq.6, what can be called the *frequency-to-failure*, to highlight where the failure should start first, as in Fig.5 by brighter tones on higher log Z axis.

5. Defect tolerance based on full-field dynamic testing & Risk Index

With the *experiment-based time-to-failure maps* we can build a *defect tolerance*, in manufacturing as well as in exercise, based on the real dynamics and a *Risk Index* definition of our choice. From the *fatigue spectral methods* on

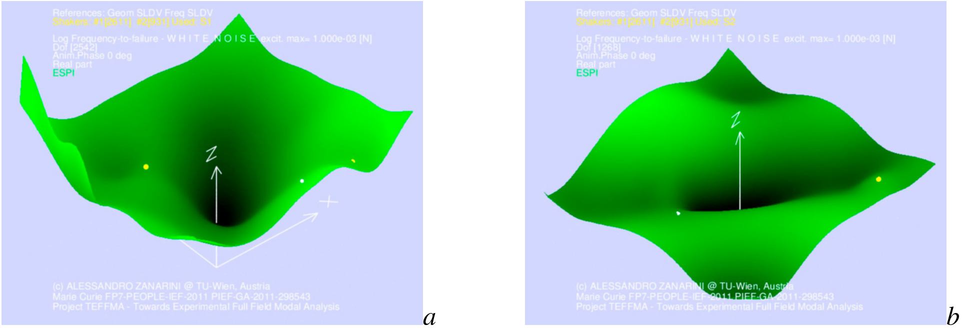

Fig. 5. Examples of *frequency-to-failure distribution* maps from *white noise excitation*, ESPI examples: from shaker 1 in *a*, from shaker 2 in *b*.

experimental full-field data, as an example, a ***Risk Index*** can be proposed, which is based on the *Hours_to_Failure*:

$$T_{failure_{[dof]}} = \frac{K_r}{\left(F_{p[dof]} S^{b}_{eq[dof]}\right)} \rightarrow Hours\_to\_Failure_{[dof]} = HtF_{[dof]}, \tag{7}$$

and can be defined in every dof, in a decibel shape, relative to the *mean* of *HtF* distribution:

$$RiskIndex_{[dof]} = 20log_{10}(\frac{1}{HtF_{[dof]}}) - 20log10(\frac{1}{HtF_{mean}}). \tag{8}$$

Therefore we can speak about the *defect tolerance* as proportional to the defined *Risk Index*, putting a *threshold* of acceptance: **defect tolerance** α **Risk Index**, e.g. safety achieved when $RiskIndex_{[dof]} \leq threshold$.

The concept can be expanded by any different *coloured noise excitation*, or also by a *real measured force*, to evaluate the related *VonMises equivalent stress PSDs*. Different *PSDs* bring their respective *Risk Index maps*. In the examples of Fig.6 the location of the magenta dof, with a *threshold* of 10, gives the information if, according to the proposed *Risk Index*, the potential defect is tolerable or not, with clear safety repercussions in production or exercise. Also in the examples of Fig.7, obtained instead with a *pink noise excitation* from shaker 1, where the *Risk Index maps*

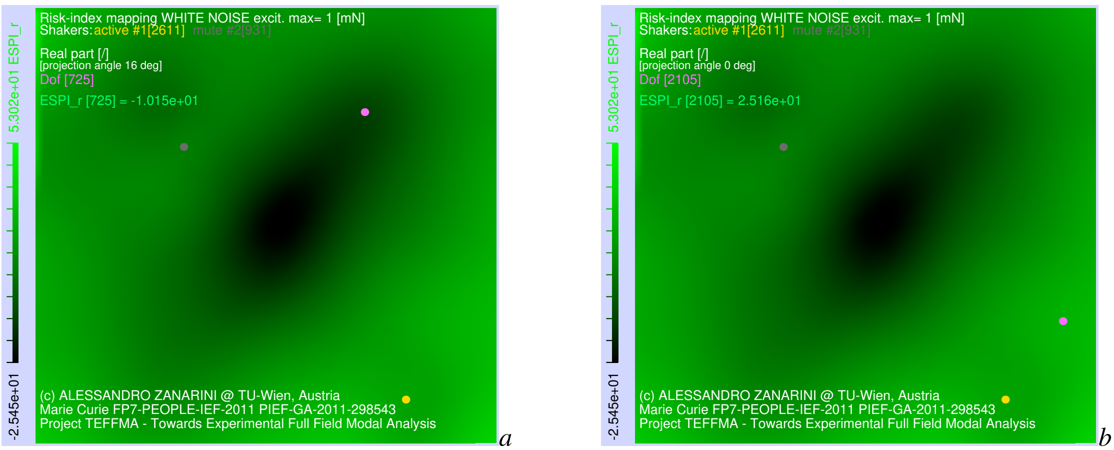

Fig. 6. Examples of *Risk Index mapping* in dof 725 in *a* and 2105 in *b*, with *white noise excitation* from shaker 1. If $threshold = 10$, a defect in dof 725 is tolerable, whereas a defect in dof 2105 is intolerable, thus dangerous.

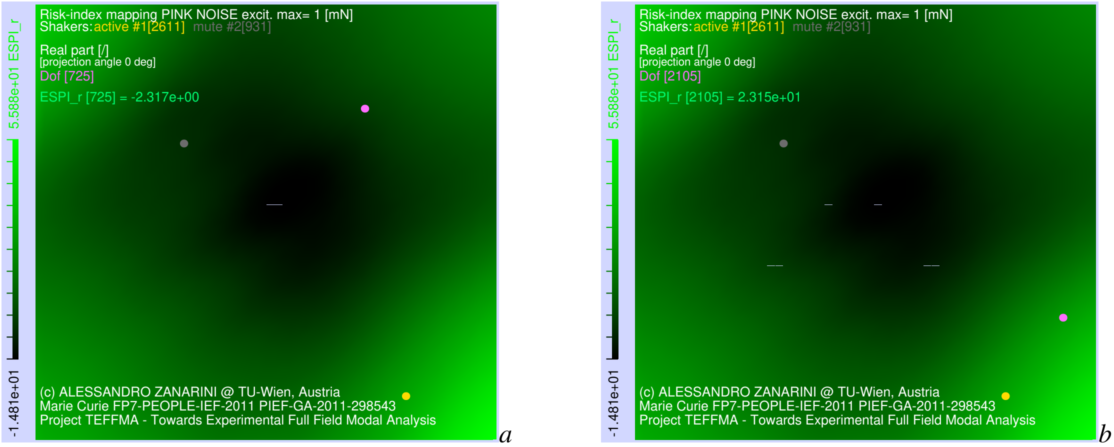

Fig. 7. Examples of *Risk Index mapping* in dof 725 in *a* and 2105 in *b*, with *pink noise excitation* from shaker 1. If *threshold* = 10, a defect in dof 725 is tolerable, whereas a defect in dof 2105 is intolerable, thus dangerous.

are completely different due to the lower emphasis on higher frequency contributions, the location of the enquiry dof can tell when it is located in a more or less dangerous zone, compared to the chosen *threshold* in Eq.8. This to underline the effectiveness of *full-field FRF based Risk Index mapping*: it was sufficient to change the *dynamic signature* of the excitation to understand how the problematic areas on the sample changed.

The *damage location assessment* on real components may play a relevant role under the *defect tolerance strategies*. The chosen 2 dofs above were just a virtual example, but the same ESPI-based *NDT* shown in paper Zanarini (2021a) may give us a *real defect distribution map*, which can be the input in *Risk Index maps*, here obtained by ESPI full-field dynamic testing in Zanarini (2021b), both for production & exercise of our parts. In this coupled strategy, the real location of the defect can tell if it can be accepted or not, in manufacturing or exercise, once the real structural dynamics and excitation signature are fully known. Therefore the *NDT*, the *structural dynamics'* measurement and the *defect tolerance criteria* can all be based on *full-field dynamic testing*, to put the most advanced experimental structural dynamics' knowledge into higher safety targets.

6. Conclusions

Many activities were run before being able to pursue the final goal of a methodologically sound *risk tolerance assessment*. Among them, it's important to recall: the extended tests to acquire high quality *full-field FRFs* for NVH & advanced design procedures; the accurate evaluation of *Strain FRF maps* from *experimental full-field receptances*; the evaluation of *Stress & Von Mises equivalent stress FRF maps* with proper constitutive models; the simulation of *Von Mises PSDs* directly from *experimental full-field FRFs* and *coloured noise excitation*; the *fatigue life predictions* by means of *spectral methods*, with *full-field impedance-based experimental models*; and the definition of a *Risk Index* to discriminate the dangerous location of defects, once the real dynamic behaviour is fully retained and not simplified.

It is now possible to state that the experimental optical full-field measurement techniques are becoming mature & reliable for a *risk tolerance assessment* in production and working conditions, because of their ability to identify defects and to retain a refined structural dynamics in both the frequency and spatial domain, directly from real samples and without any FE model to be carefully updated.

Acknowledgements

The European Commission Research Executive Agency is acknowledged for funding the project TEFFMA - Towards Experimental Full Field Modal Analysis, funded by the European Commission at the Technische Universitaet Wien, Austria, through the Marie Curie FP7-PEOPLE-IEF-2011 PIEF-GA-2011-298543 grant in years 2013-2015.

References

T. Dirlik. *Application of computers in fatigue analysis*. PhD thesis, University of Warwick, January 1985. URL http://wrap.warwick.ac.uk/2949/.

T. Dirlik and D. Benasciutti. Dirlik and Tovo-Benasciutti Spectral Methods in Vibration Fatigue: A Review with a Historical Perspective. *Metals*, 11(9), 2021. ISSN 2075-4701. https://doi.org/10.3390/met11091333. URL https://www.mdpi.com/2075-4701/11/9/1333.

A. Zanarini. Dynamic behaviour carachterization of a brake disc by means of electronic speckle pattern interferometry measurements. In *Proceedings of the IDETC/CIE ASME International Design Engineering Technical Conferences & Computers and Information in Engineering Conference, Long Beach, California, USA, September 24-28*, pages 273–280. ASME, 2005a. https://doi.org/10.1115/DETC2005-84630. Paper DETC2005-84630.

A. Zanarini. Damage location assessment in a composite panel by means of electronic speckle pattern interferometry measurements. In *Proceedings of the IDETC/CIE ASME International Design Engineering Technical Conferences & Computers and Information in Engineering Conference, Long Beach, California, USA, September 24-28*, pages 1–8. ASME, 2005b. https://doi.org/10.1115/DETC2005-84631. Paper DETC2005-84631.

A. Zanarini. Full field ESPI measurements on a plate: challenging experimental modal analysis. In *Proceedings of the XXV IMAC, Orlando (FL) USA, Feb 19-22*, pages 1–11. SEM, 2007. URL https://www.researchgate.net/publication/266896551_Full_field_ESPI_measurements_on_a_plate_Challenging_Experimental_Modal_Analysis. Paper s34p04.

A. Zanarini. Fatigue life assessment by means of full field ESPI vibration measurements. In P. Sas, editor, *Proceedings of the ISMA2008 Conference, September 15-17, Leuven (Belgium)*, pages 817–832. KUL, 2008a. https://doi.org/10.13140/RG.2.1.3452.9365. Condition monitoring, Paper 326.

A. Zanarini. Full field ESPI vibration measurements to predict fatigue behaviour. In *Proceedings of the IMECE2008 ASME International Mechanical Engineering Congress and Exposition, October 31- November 6, Boston (MA) USA*, pages 165–174. ASME, October 31- November 6 2008b. https://doi.org/10.1115/IMECE2008-68727. Paper IMECE2008-68727.

A. Zanarini. On the estimation of frequency response functions, dynamic rotational degrees of freedom and strain maps from different full field optical techniques. In *Proceedings of the ISMA2014 including USD2014 - International Conference on Noise and Vibration Engineering, Leuven, Belgium, September 15-17*, pages 1177–1192. KU Leuven, September 15-17 2014a. URL http://past.isma-isaac.be/downloads/isma2014/papers/isma2014_0676.pdf. Dynamic testing: methods and instrumentation, paper ID676.

A. Zanarini. On the role of spatial resolution in advanced vibration measurements for operational modal analysis and model updating. In *Proceedings of the ISMA2014 including USD2014 - International Conference on Noise and Vibration Engineering, Leuven, Belgium, September 15-17*, pages 3397–3410. KU Leuven, September 15-17 2014b. URL http://past.isma-isaac.be/downloads/isma2014/papers/isma2014_0678.pdf. Operational modal analysis, paper ID678.

A. Zanarini. Comparative studies on full field FRFs estimation from competing optical instruments. In *Proceedings of the ICoEV2015 International Conference on Engineering Vibration, Ljubljana, Slovenia, September 7-10*, pages 1559–1568. Univ. Ljubljana & IFToMM, September 7-10 2015a. URL https://www.researchgate.net/publication/280013709_Comparative_studies_on_Full_Field_FRFs_estimation_from_competing_optical_instruments. ID191.

A. Zanarini. Accurate FRFs estimation of derivative quantities from different full field measuring technologies. In *Proceedings of the ICoEV2015 International Conference on Engineering Vibration, Ljubljana, Slovenia, September 7-10*, pages 1569–1578. Univ. Ljubljana & IFToMM, September 7-10 2015b. URL https://www.researchgate.net/publication/280013778_Accurate_FRF_estimation_of_derivative_quantities_from_different_full_field_measuring_technologies. ID192.

A. Zanarini. Full field experimental modelling in spectral approaches to fatigue predictions. In *Proceedings of the ICoEV2015 International Conference on Engineering Vibration, Ljubljana, Slovenia, September 7-10*, pages 1579–1588. Univ. Ljubljana & IFToMM, September 7-10 2015c. URL https://www.researchgate.net/publication/280013788_Full_field_experimental_modelling_in_spectral_approaches_to_fatigue_predictions. ID193.

A. Zanarini. Model updating from full field optical experimental datasets. In *Proceedings of the ICoEV2015 International Conference on Engineering Vibration, Ljubljana, Slovenia, September 7-10*, pages 773–782. Univ. Ljubljana & IFToMM, September 7-10 2015d. URL https://www.researchgate.net/publication/280013876_Model_updating_from_full_field_optical_experimental_datasets. ID196.

A. Zanarini. Broad frequency band full field measurements for advanced applications: Point-wise comparisons between optical technologies. *Mechanical Systems and Signal Processing*, 98:968 – 999, 2018. ISSN 0888-3270. https://doi.org/10.1016/j.ymssp.2017.05.035.

A. Zanarini. Competing optical instruments for the estimation of Full Field FRFs. *Measurement*, 140:100 – 119, 2019a. ISSN 0263-2241. https://doi.org/10.1016/j.measurement.2018.12.017.

A. Zanarini. Full field optical measurements in experimental modal analysis and model updating. *Journal of Sound and Vibration*, 442:817 – 842, 2019b. ISSN 0022-460X. https://doi.org/10.1016/j.jsv.2018.09.048.

A. Zanarini. On the making of precise comparisons with optical full field technologies in NVH. In *Proceedings of the ISMA2020 including USD2020 - International Conference on Noise and Vibration Engineering, Leuven, Belgium, September 7-9*, pages 2293–2308. KU Leuven, September 7-9 2020. URL https://www.researchgate.net/publication/344353185_On_the_making_of_precise_comparisons_with_optical_full_field_technologies_in_NVH. Optical methods and computer vision for vibration engineering, paper ID 695.

A. Zanarini. On the exploitation of multiple 3D full-field pulsed espi measurements in damage location assessment. *Procedia Structural Integrity*, pages 1–8, 2021a. ISSN 2452-3216. paper ID 104, ICSI 2021 The 4th International Conference on Structural Integrity.

A. Zanarini. On the defect tolerance by fatigue spectral methods based on full-field dynamic testing. *Procedia Structural Integrity*, pages 1–8, 2021b. ISSN 2452-3216. paper ID 105, ICSI 2021 The 4th International Conference on Structural Integrity.

A. Zanarini. Chasing the high-resolution mapping of rotational and strain FRFs as receptance processing from different full-field optical measuring technologies. *Mechanical Systems and Signal Processing*, page 108428, 2021c. ISSN 0888-3270. https://doi.org/10.1016/j.ymssp.2021.108428.